Organic & Biomolecular Chemistry

Cite this: *Org. Biomol. Chem.*, 2011, **9**, 2473

www.rsc.org/obc

PAPER

DEPMPO: an efficient tool for the coupled ESR-spin trapping of alkylperoxyl radicals in water†‡

Hakim Karoui,* Florence Chalier, Jean-Pierre Finet and Paul Tordo*

Received 13th October 2010, Accepted 13th December 2010
DOI: 10.1039/c0ob00876a

Peroxidation is an important process both in chemistry and biology, and peroxyl radicals play a crucial role in various pathological situations involving lipid and protein peroxidation. A few secondary and tertiary peroxyl radicals can be detected directly by Electron Spin Resonance (ESR). However, primary and secondary alkylperoxyl radicals have extremely short lifetimes and their direct observation is impossible in biological samples. DMPO has been used to trap alkylperoxyl radicals generated in biological systems and the characterization of DMPO–alkylperoxyl spin adducts has been claimed by different authors. However, it was then clearly shown that all the assignments made previously to DMPO–OOR adducts were actually due to DMPO–OR adducts. We have investigated the potential of DEPMPO to characterize the formation of alkylperoxyl radicals in biological milieu. Various DEPMPO–OOR (R = Me, primary or secondary alkyl group) spin adducts were unambiguously characterized and the formation of DEPMPO–$OOCH_3$ was clearly established during the reaction of *tert*-butylhydroperoxide with chloroperoxidase and cytochrome c.

Introduction

The main physiological source of peroxyl free radicals comes from radical chain reactions involving polyunsaturated fatty acids (PUFA) and molecular oxygen. The generated lipid peroxyl and lipid alkoxyl radicals are responsible for lipid peroxidation which could lead to membrane destruction followed by cell death. Lipid peroxyl radicals are also involved in protein and DNA damage,[1,2] contributing to pathological situations such as atherosclerosis[3] and neurodegenerative diseases.[4,5]

In 1980's, several groups reported the observation and the characterization of tertiary alkylperoxyl and secondary lipid-derived peroxyl radicals using direct Electron Spin Resonance (ESR) spectroscopy at room temperature.[6] However, due to fast disproportionation primary and secondary alkylperoxyl free radicals can not be observed directly in biological systems. The use of ESR in conjunction with the spin trapping technique has become an important tool for detecting transient free radicals and this approach has been widely used to trap oxygen-centered free radicals.[7–9] DMPO is a popular spin trap (Scheme 1), although this trap is not without limitations. By reaction with superoxide at physiological pH, it yields the DMPO–OOH spin adduct which exhibits a very short lifetime ($t_{1/2} \approx$ 50 s) thus making close to impossible the characterization of superoxide in biological milieu. Furthermore, once it is formed, DMPO–OOH decomposes rapidly to the persistent hydroxyl adduct (DMPO–OH), leading to misinterpretations of the spin trapping experiments.[10] In the literature, many papers reported the trapping with DMPO of alkylperoxyl free radicals generated during the decomposition of organic hydroperoxides by various heme proteins.[4,11–18] Identification of DMPO–peroxyl spin adducts was based only on the similarity between their ESR spectra and that of the superoxide adduct DMPO–OOH, in conjunction with their insensitivity to superoxide dismutase (SOD). However, in 1999 using $^{17}O_2$, Dikalov and Mason established that most of the assignments to DMPO–OOR adducts were wrong and should be reassigned to DMPO–OR adducts.[19] Concerning the trapping of peroxyl radicals resulting from polyunsaturated fatty acids (PUFA) oxidation, these authors reassigned also the DMPO–OOPUFA spin adducts to DMPO–OPUFA adducts.[20]

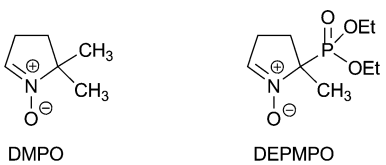

Scheme 1 Spin trap structures.

Using ESR continuous-flow experiments, Jones and Burkitt showed that DMPO can trap *tert*-butylperoxyl radical; however

Universités d'Aix-Marseille I, II et III - CNRS UMR 6264. Laboratoire Chimie Provence, Equipe SREP, 13397 Marseille, Cedex 20, France. E-mail: hakim.karoui@univ-provence.fr, paul.tordo@univ-provence.fr; Fax: +33 4 91 28 87 58; Tel: +33 4 91 28 86 10

† This work is dedicated to the memory of Athel Beckwith, a teacher and scientist from whom we learned how to study chemistry by example. His pioneering advances in radical chemistry laid the foundation for much of the current radical clock methodology.

‡ Electronic supplementary information (ESI) available: ESR spectra. See DOI: 10.1039/c0ob00876a

the resulting adduct was too unstable to be easily characterized by EPR.[21]

In the past decade, DEPMPO (Scheme 1) has been successfully used for the *in vivo* detection of oxygen-centered radicals.[8,22–27] The high persistency of the superoxide spin adduct at physiological pH ($t_{1/2} \approx 900$ s) and its insignificant spontaneous decomposition to the hydroxyl adduct or other paramagnetic by-products are the main advantages of using DEPMPO.[28] The ESR spectrum of the DEPMPO–OOH adduct is a superimposition of two different signals corresponding to the *cis* and *trans* diastereoisomeric adducts in a 1 to 9 ratio respectively. The main signal is characterized by an alternating line width phenomenon, attributed to a chemical exchange between 2 conformational sites (T_1 and T_2) of the *trans* diastereoisomer with different ESR coupling constants (Fig. 1a). In organic solvents the *tert*-butylperoxyl radical is trapped efficiently by DEPMPO[29] and in toluene, at room temperature, the ESR signal of the DEPMPO–OO-*tert*-Bu adduct lasted more than one hour.

In our original paper on the synthesis and use of DEPMPO as a spin trap, we reported the trapping of methylperoxyl radical with DEPMPO in water.[22] Later, Clément *et al.* showed that DEPMPO is able to trap the protein-peroxyl radicals generated from the reaction of bovine serum albumin (BSA) and hydroxyl radical in oxygen-saturated buffer.[30] However, the very close similitude of the EPR spectra of DEPMPO–OOH and DEPMPO-OOMe[22] and the reassignments performed by Dikalov *et al.* in the case of the DMPO–alkylperoxyl adducts led us to question our preliminary claims and to fully investigate the trapping of various alkylperoxyl radicals (ROO$^{\bullet}$) with DEPMPO in water, our results are reported herein.

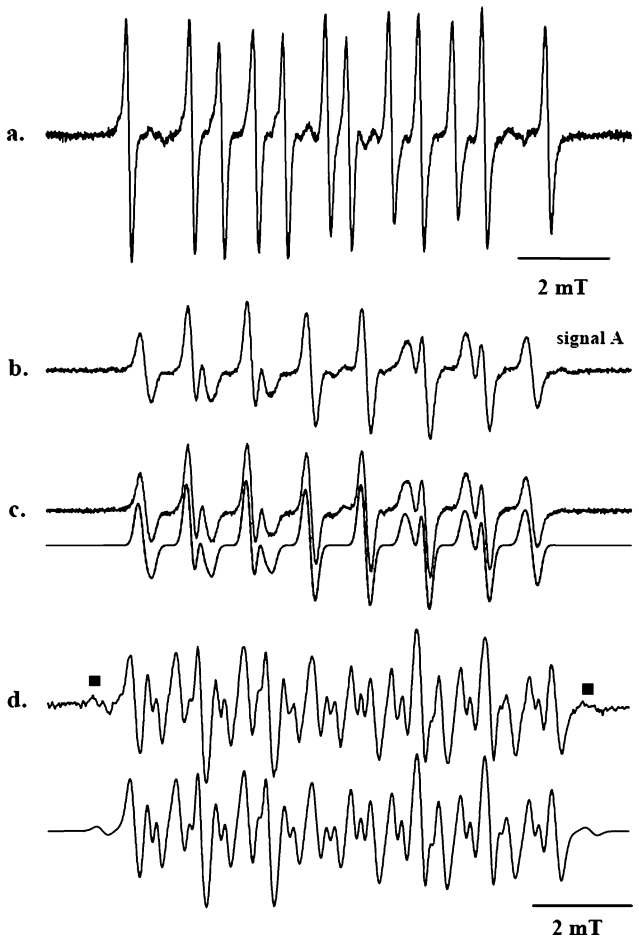

Fig. 1 DEPMPO-OOCH$_3$ spin adduct generation. a, UV-photolysis of a solution containing DEPMPO (5 mM), H_2O_2 (1%) and DMSO (10%) in deoxygenated phosphate buffer (0.1 M, pH 7.4), **b**, UV-photolysis of a solution containing DEPMPO (5 mM), H_2O_2 (1%) and DMSO (10%) in O_2-saturated phosphate buffer (0.1 M, pH 7.4), **c.** as (**b**) but in the presence of SOD (0.1 mg mL^{-1}). **d.** DEPMPO–OCH$_3$ spin adduct. It was obtained by incubating $FeCl_3$ (2 mM) in a methanolic solution of DEPMPO (0.5 M) for 2 min; then 30 μL of this solution were added to 270 μL of a phosphate buffer solution (0.1 M, pH 7.4) containing DTPA (20 mM). The signal below represents the computer simulation and the filled square (■) a paramagnetic impurity. Spectrometer settings: microwave power, 10 mW; modulation amplitude, 0.1 mT (0.05 mT for **d**.); time constant, 0.128 s; gain, 5×10^4; scan range, 14 mT (12 mT for **d**.) and scan time, 43 s (4 scans). All the given concentrations are final concentrations in the reaction mixture.

Results and discussion

Trapping of ROO$^{\bullet}$ (R = Me, *n*-Bu, *i*-Pr) generated from the reaction between HO$^{\bullet}$ and dialkylsulfoxides (R_2SO) in the presence of oxygen

UV-photolysis of a phosphate buffer solution containing hydrogen peroxide (H_2O_2) and dimethylsulfoxide (DMSO) constitutes a useful system to generate methyl radicals. In the absence of oxygen and in the presence of DEPMPO (5 mM), the expected 12 line signal of the DEPMPO–CH_3 spin adduct[22] was observed (Fig. 1a). In the presence of oxygen, the methyl radical reacts with oxygen at a nearly diffusion-controlled rate to generate $CH_3OO^{\bullet}$ and a completely different ESR signal (signal A, Fig. 1b) showing a general pattern similarity with the DEPMPO–OOH adduct (see Electronic Supplementary Information, Figure S1a‡) was observed.

The same experiment was repeated in the presence of SOD to prevent the formation of DEPMPO–OOH (see Electronic Supplementary Information, Figure S1b) and to rule out the assignment of signal A in Fig. 1b to DEPMPO–OOH. After checking that a sample of SOD irradiated during 20 min retained its activity (see Electronic Supplementary Information, Figure S1c), we showed that a high concentration of SOD (500 U mL^{-1}) does not affect signal A (see Electronic Supplementary Information, Figure S1c). As expected, in the absence of DMSO, acting as the source of methyl radicals, only the DEPMPO–OH spin adduct was clearly observed (see Electronic Supplementary Information, Figure S1d). Identical results were obtained when hydroxyl radicals were generated *via* a Fenton system (H_2O_2/Fe^{2+}).

To avoid the risk of misassignment of signal A, an authentic DEPMPO–OCH_3 spin adduct was generated by the nucleophilic addition of MeOH to DEPMPO (Fig. 1d). Its ESR spectrum was completely different from signal A. An excellent fit was obtained for the simulation assuming the presence of *cis* and *trans* DEPMPO–OCH_3 diastereoisomers, with different ESR coupling constants (Table 1) and an additional minor signal corresponding to a paramagnetic impurity (■). Thus, the ESR signal A can be unambiguously assigned to the DEPMPO–$OOCH_3$ spin adduct, and it was satisfactorily simulated assuming the presence of two

Table 1 ESR coupling constants of numerous DEPMPO spin adducts

			ESR parameters of the spin adduct						
Radical spin adduct	Radical source	Solvent	% dia[d]	% conf	a_N/mT	$a_{H\beta}$/mT	a_P/mT	$a_{H\gamma}$/mT	k^a/s $\times 10^{-7}$
DEPMPO–OOH	HY/XO	water[b]	*trans* 90	$\mathbf{T_1}$ 50[c]	1.31	1.2	5.12	0.09	8
				$\mathbf{T_2}$ 50[c]	1.30	1.0	4.86	0.09	
			cis 10		1.34	0.90	4.06		
DEPMPO–$OOCH_3$	H_2O_2/O_2 DMSO/hν	water[b]	*trans*	$\mathbf{T_1}$ 52[c]	1.34	0.90	4.80		1.5
				$\mathbf{T_2}$ 48[c]	1.31	1.15	5.00		
	tert-BuOOH/chloroperoxidase	water[b]	*trans*	$\mathbf{T_1}$ 52[c]	1.32	0.87	4.90	0.06	0.5
				$\mathbf{T_2}$ 48[c]	1.32	1.14	5.00	0.07	
	Cyt C/O_2/*tert*-BuOOH	water[b]	*trans*	$\mathbf{T_1}$ 51[c]	1.34	0.90	4.81		2.1
				$\mathbf{T_2}$ 49[c]	1.32	1.16	5.03		
DEPMPO–OO*n*-Bu	H_2O_2/O_2 *n*-Bu_2SO/hν	water[b]	*trans*	$\mathbf{T_1}$ 59[c]	1.30	0.95	4.79	0.10	2.9
				$\mathbf{T_2}$ 41[c]	1.30	1.20	5.20	0.09	
DEPMPO–OO*i*-Pr	H_2O_2/O_2 *i*-Pr_2SO/hν	water[b]	*trans*	$\mathbf{T_1}$ 58[c]	1.30	0.96	4.80	0.10	2.9
				$\mathbf{T_2}$ 42[c]	1.32	1.18	5.20	0.09	
DEPMPO–OOL	Cyt C/LOOH	water[b]	*trans*	$\mathbf{T_1}$ 64[c]	1.21	1.09	5.27		4.8
				$\mathbf{T_2}$ 36[c]	1.23	0.72	4.29		
DEPMPO–OH	$H_2O_2/FeSO_4$	water[b]			1.40	1.32	4.71		
	Cyt c/LOOH	water[b]			1.39	1.37	4.73		
DEPMPO–OCH_3	CH_3OH/Fe^{3+} + PB[b]	water[b]	*trans* 59.8		1.35	0.92	4.77	0.09	
			cis 40.2		1.37	0.82	4.07	0.18	
DEPMPO–O*n*-Bu	*n*-BuOH/Fe^{3+} + PB[b]	water[b]	*trans* 57.9		1.36	0.91	4.79		
			cis 42.1		1.38	0.86	4.07		
DEPMPO–O*i*-Pr	*i*-PrOH/Fe^{3+} + PB[b]	water[b]	*trans* 70.2		1.38	1.00	4.72		
			cis 29.8		1.40	0.97	4.20		
DEPMPO–O*tert*-Bu	(*tert*-BuO)$_2$/*hν* +PB[b]	water[b]			1.39	1.46	4.65		
	(*tert*-BuO)$_2$/*hν*	*tert*-BuOH			1.33	0.89	4.69		
DEPMPO–OAAPH	AAPH/*hν*	water[b]			1.37	1.29	4.61		
DEPMPO–L	Cyt c/LOOH	water[b]			1.49	2.24	4.77		
DEPMPO–CH_3	H_2O_2/DMSO/*hν*	water[b]			1.52	2.23	4.77		

[a] Exchange rate. [b] 0.1 M phosphate buffer, pH 7.4. [c] Percentage contribution of conformer. [d] Percentage contribution of diastereoisomer.

exchanging conformational sites with different coupling constants (Fig. 1c and Table 1).

The trapping of primary (*n*-BuOO$^\bullet$) and secondary (*i*-PrOO$^\bullet$) peroxyl radicals was also investigated to observe the effect of alkyl substitution on the efficiency of DEPMPO to trap peroxyl radicals. *n*-BuOO$^\bullet$ and *i*-PrOO$^\bullet$ were obtained by irradiation of an oxygen-saturated phosphate buffer solution of the corresponding dialkylsulfoxide (*n*-Bu_2SO and *i*-Pr_2SO) in the presence of hydrogen peroxide (H_2O_2) and DEPMPO. The observed ESR spectra (Fig. 2) presented a characteristic alternating line width phenomenon and exhibited a general pattern similar to that of DEPMPO–$OOCH_3$. These spectra were satisfactorily simulated considering two conformational sites in a chemical exchange and with different ESR coupling constants (Table 1). Because of the similarity of these ESR spectra with that of DEPMPO-OOMe, they were assigned to the *trans* diastereoisomers of DEPMPO-OO*n*-Bu or DEPMPO-OO*i*-Pr. Authentic spectra of DEPMPO-O*n*-Bu and DEPMPO-O*i*-Pr spin adducts were generated independently by nucleophilic addition of ROH on DEPMPO catalyzed by Fe^{3+} and dilution of the respective samples in phosphate buffer (0.1 M, pH 7.4) containing DTPA (20 mM) to avoid nucleophilic addition of water (Electronic Supplementary Information, Figure S2a and b, respectively). Their ESR signals are different in water than those assigned to the corresponding peroxyl radical adducts given in Fig. 3. DEPMPO-O*n*-Bu and DEPMPO-O*i*-Pr spin adducts exhibit ESR spectra resulting from the presence of *cis* and *trans* diastereoisomers with different coupling constants (Table 1). Additional and wider signals were observed, simulated and attributed to carbon-centered radicals (⊙, a_N = 1.49; a_H = 2.17 and a_P = 4.86 mT) and (*, a_N = 1.47; a_H = 2.06 and a_P = 4.76 mT) (Electronic Supplementary Information, Figure S2a and b, respectively‡).

Trapping of tertiary alkylperoxyl radicals

In organic solvents, we showed that DEPMPO–OO*tert*-Bu can be easily detected over a large temperature range.[29] However, all our attempts to detect this adduct in phosphate buffer, generating the *tert*-butylperoxyl radical by photolytic cleavage of *tert*-BuOOH in the presence of DEPMPO failed. So we decided to generate a tertiary alkyl peroxyl radical by the photolytic cleavage of 2,2′-azobis-2-methylpropionamidine hydrochloride (AAPH) in phosphate buffer. When a solution of AAPH (5 mM) in O_2-saturated phosphate buffer (0.1 M, pH 7.4) was decomposed by photolysis in the presence of DEPMPO (50 mM), only an intense doublet of quadruplets (a_N = 1.37; a_H = 1.29 and a_P = 4.61 mT) characteristic of the trapping of a tertiary alkoxyl radical, likely the protonated 2-methylpropionamidinoxyl radical $[Me_2C(O^\bullet)C(NH_2)_2]^+$, was observed.[31] Varying the concentrations of the reactants resulted only in the change of the signal intensity. However, when the reaction mixture was carefully deoxygenated only the signal of the $[DEPMPO–C(Me)_2C(NH_2)_2]^+$ adduct was observed. In the presence of oxygen, the carbon centered radical $[^\bullet C(Me)_2C(NH_2)_2]^+$ resulting from the photolytic cleavage of AAPH is trapped by O_2 to form the protonated 2-methylpropionamidinylperoxyl radical (AAPH–OO$^\bullet$) which can either form the corresponding tetraoxide (AAPH–OOOO–HPAA) or add to DEPMPO to form DEPMPO–OOHPAA (Scheme 2). Then, the tetraoxide is expected

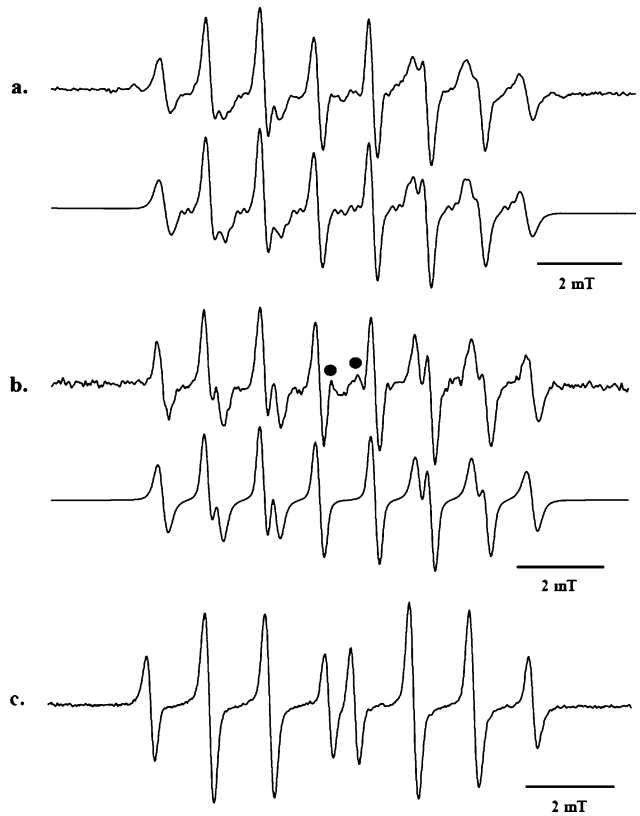

Fig. 2 DEPMPO–primary and secondary peroxyl and alkoxyl spin adducts formation in water. **a**, DEPMPO–OO*n*-Bu ESR spectrum was obtained upon continuous irradiation of an incubation mixture containing DEPMPO (50 mM), hydrogen peroxide (1% v/v) and di-*n*-butyl sulfoxide (0.5 M) in oxygenated phosphate buffer (0.1 M, pH 7.4). The spectrum below represents the computer simulation. **b**, DEPMPO-OO*i*-Pr formation using the same conditions than **a.** but with diisopropyl sulfoxide (0.5 M). The spectrum below represents the computer simulation. **c**, UV-photolysis of an incubation mixture containing DEPMPO (25 mM), AAPH (10 mM) in oxygen-saturated phosphate buffer (0.1 M, pH 7.4). Spectrometer settings: microwave power, 10 mW (20 mW in the case of **c.**); modulation amplitude, 0.05 mT (0.1 mT for **c.**); time constant, 0.128 s; gain, 10^5; scan range, 14 mT (12 mT for **c.**) and scan time, 168 s (83 s and 4 scans in the case of **b.**).

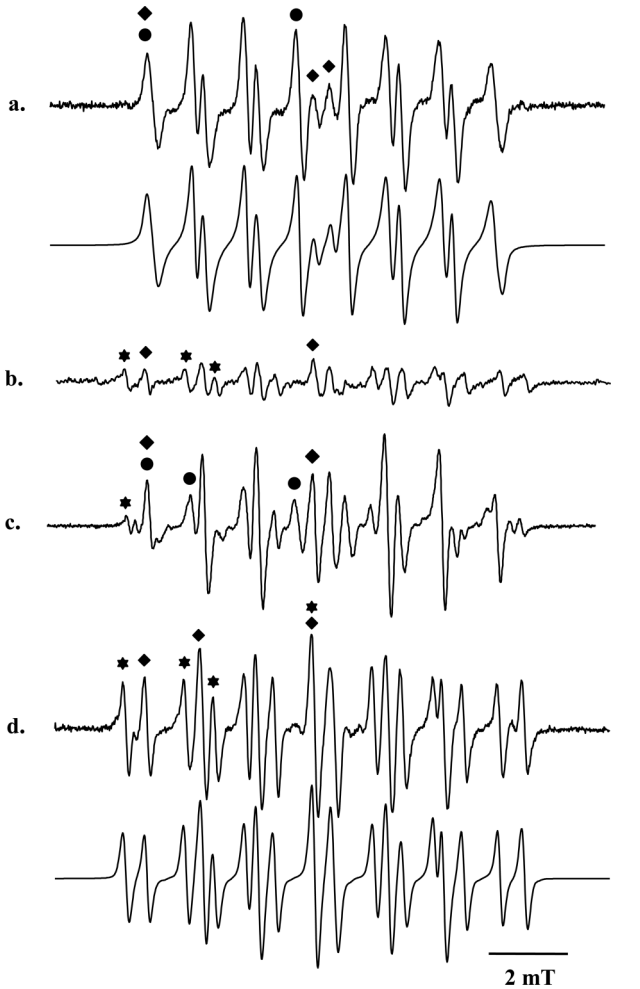

Fig. 3 Free radicals trapped during the reaction between cytochrome c and *tert*-BuOOH. a, incubation of cytochrome c (20 μM) with a solution of *tert*-BuOOH (15 mM), DTPA (0.3 mM) and DEPMPO (5 mM) in oxygen-saturated phosphate buffer (0.1 M, pH 7.4). The signal below represents the computer simulation assuming the presence of 2 exchanging conformers of DEPMPO–$OOCH_3$ (●) and DEPMPO–O*tert*-Bu (◆). b, as (a) but in the absence of oxygen realized by bubbling argon in the incubation mixture; c, as (b) but DEPMPO (50 mM); d, as (a) but in the presence of DEPMPO (50 mM) in degassed phosphate buffer (0.1 M, pH 7.4). The spectrum below is the computer simulation of the experimental signal assuming the presence of 2 different species, the DEPMPO–CH_3 (★) and DEPMPO-O*tert*-Bu (◆). Spectrometer settings: microwave power, 10 mW; modulation amplitude, 0.1 mT; time constant, 0.128 s; gain, 1×10^5; scan range, 14 mT and scan time, 43 s (2 scans for each signal).

to decompose to O_2 and AAPHO$^{\bullet}$ radicals which are trapped by excess DEPMPO, and furthermore, like DMPO–OO*tert*-Bu, the [DEPMPO-OOHPAA] adduct is proposed to undergo rapid degradation with liberation of the free AAPHO$^{\bullet}$ radicals which again are trapped by the excess of DEPMPO (Fig. 2c).

Trapping of oxygen centered radicals generated by the *tert*-BuOOH–cytochrome c system. The reaction of a mixture containing cytochrome c (20 μM), *tert*-BuOOH (15 mM), DTPA (0.3 mM) and DEPMPO (5 mM) in oxygen-saturated phosphate buffer (0.1 M, pH 7.4) gave the ESR spectrum shown in Fig. 4a. This signal was not affected by the presence of SOD (500 U mL^{-1}) (data not shown) which rules out the trapping of superoxide. The signal in Fig. 3a was satisfactorily simulated assuming the presence of two different signals: one attributed to a DEPMPO–peroxyl spin adduct and the other to a DEPMPO–alkoxyl spin adduct. From their ESR parameters, the former was assigned to DEPMPO–OOMe and the later to DEPMPO–O*tert*-Bu in agreement with the experimental conditions used and the mechanism of the *tert*-butylperoxyl radical decomposition (Scheme 3, eqn (4) to (6)). The simulated spectrum was obtained considering 90 and 10% contributions of two exchanging conformational sites of DEPMPO–OOMe (●, Fig. 3a) and DEPMPO–O*tert*-Bu (◆, Fig. 3a) (Table 1). Our assignments were supported by the results observed when the reaction was repeated after bubbling argon to deoxygenate the incubation mixture. In the absence of oxygen the formation of MeOO$^{\bullet}$ is cancelled and the signal obtained corresponded to a mixture of *tert*-butoxyl (◆, Fig. 3b) and methyl adducts (★, Fig. 3b).

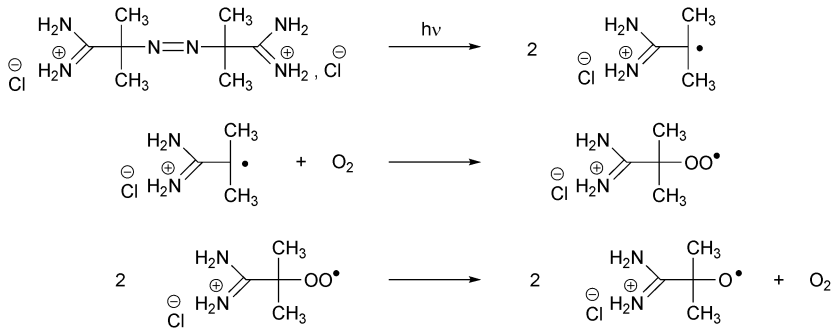

Scheme 2 Mechanism of AAPH decomposition.

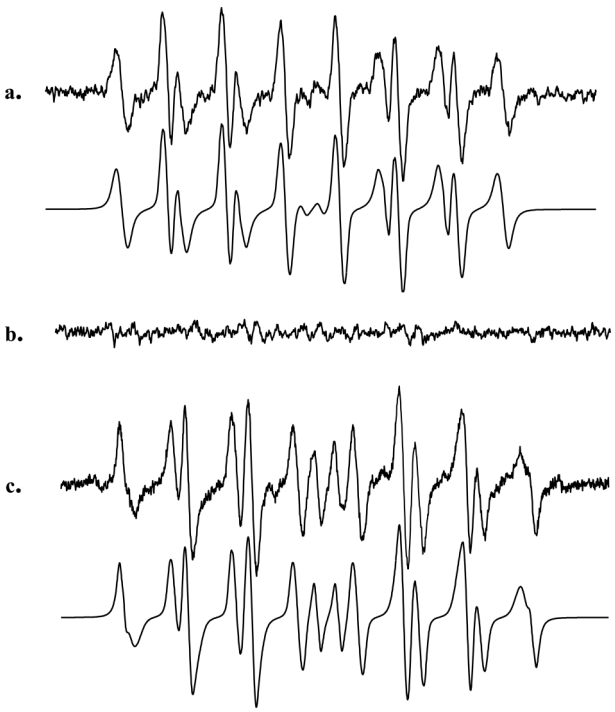

Fig. 4 Spectra of DEPMPO adducts formed in *tert*-BuOOH–chloroperoxidase system. **a**, incubation of chloroperoxidase (10 U.mL^{-1}) (4 min) in a reaction mixture containing *tert*-BuOOH (60 mM) and DEPMPO (10 mM) in oxygenated phosphate buffer (0.1 M, pH 7.4); simulation by superimposition of DEPMPO–OOMe (95%) and DEPMPO–O*tert*-Bu (5%). **b**, as (**a**) but in absence of oxygen, **c**, as (**a**) but DEPMPO was 100 mM. The spectrum below represents the simulation assuming the presence of DEPMPO–OOMe (60%) and DEPMPO–O*tert*-Bu (40%). Spectrometer settings: microwave power, 10 mW modulation amplitude, 0.05 mT; time constant, 0.04 s; gain, 5×10^5; scan range, 15 mT and scan time, 42 s (2 scans for each signal).

When the concentration of DEPMPO was increased to 50 mM, two main modifications were observed. First, the relative concentration of DEPMPO–OOMe fell dramatically in comparison with the concentration of DEPMPO–O*tert*-Bu, and secondly a small amount of the DEPMPO–Me adduct was now detected (★, Fig. 3c). However, no detectable DEPMPO–OMe was observed. When the latter reaction (50 mM DEPMPO) was realized in the absence of oxygen, the ESR spectrum corresponded to the superimposition of DEPMPO–O*tert*-Bu (51%) and DEPMPO–Me (49%) (Fig. 3d). The use of a higher concentration of DEPMPO (400 mM) in the absence of oxygen resulted in the observation of a spectrum corresponding to the superimposition of DEPMPO–O*tert*-Bu (85%) and DEPMPO–Me (15%) ESR signals (see Electronic Supplementary Information, Fig. S3‡). We have to notice that the signal coming from the trapping of $CH_3^{\bullet}$ is not completely abolished indicating competition between *tert*-BuO$^{\bullet}$ trapping and its decay to yield $CH_3^{\bullet}$. Results similar to those described above were obtained using cumylhydroperoxide instead of *tert*-butylhydroperoxide (see Electronic Supplementary Information, Fig. S4).

Trapping of oxygen centered radicals generated by the *t*-BuOOH–chloroperoxidase system. The usually accepted mechanism for the reaction between chloroperoxidase and *tert*-butylhydroperoxide (eqn (1) to (3); Scheme 3) involves the formation of *tert*-BuOO$^{\bullet}$.[12,32] Dimerization of *tert*-BuOO$^{\bullet}$ yields the corresponding tetraoxide which decomposes into *tert*-BuO$^{\bullet}$ radicals and molecular oxygen. Then, β-scission of *tert*-BuO$^{\bullet}$ radical yields acetone and either methyl radical or MeOO$^{\bullet}$ and MeO$^{\bullet}$ radicals in the absence or in the presence of oxygen, respectively (eqn (4) to (7), Scheme 3). In 1989, using DMPO as spin trap, Mason *et al.* reported the formation of the DMPO–OO*tert*-Bu spin adduct during the decomposition of *tert*-BuOOH with chloroperoxidase.[12] However, the main species formed under these conditions was later reassigned to the DMPO–OCH_3 adduct.[19] Incubation of a mixture of chloroperoxidase (23 μM, 10 U.mL^{-1}) and *tert*-BuOOH (60 mM) in the presence of DEPMPO (10 mM) in oxygenated phosphate buffer (0.1 M, pH 7.4) afforded an ESR spectrum (Fig. 4a) identical to the spectrum of

$$\textit{tert}\text{-BuOOH} + \text{CPO} \rightarrow \textit{tert}\text{-BuOH} + \text{CPO-I} \quad (1)$$

$$\textit{tert}\text{-BuOOH} + \text{CPO-I} \rightarrow \textit{tert}\text{-BuOO}^{\bullet} + \text{CPO-II} \quad (2)$$

$$\textit{tert}\text{-BuOOH} + \text{CPO-II} \rightarrow \textit{tert}\text{-BuOO}^{\bullet} + \text{CPO} \quad (3)$$

$$2\ \textit{tert}\text{-BuOO}^{\bullet} \rightarrow (\textit{tert}\text{-Bu-OO})_2 \rightarrow 2\ \textit{tert}\text{-BuO}^{\bullet} + O_2 \quad (4)$$

$$\textit{tert}\text{-BuO}^{\bullet} \rightarrow \text{Me}^{\bullet} + \text{acetone} \quad (5)$$

$$\text{Me}^{\bullet} + O_2 \rightarrow \text{MeOO}^{\bullet} \quad (6)$$

$$2\ \text{MeOO}^{\bullet} \rightarrow (\text{Me-OO})_2 \rightarrow 2\ \text{MeO}^{\bullet} + O_2 \quad (7)$$

Scheme 3 Formation of *tert*-BuOO$^{\bullet}$ by the chloroperoxidase–*tert*-BuOOH system and decomposition.

DEPMPO–OOMe described here above (Fig. 1b and 3a). The signal remained unchanged in the presence of a high concentration of SOD (500 U mL^{-1}) (data not shown). When the concentration of DEPMPO was increased, the signal changed dramatically and for a concentration of 100 mM it appeared as the superimposition of the original signal with a second signal composed of a doublet of quartets (Fig. 4c). If we assume that with DEPMPO the trapping of *tert*-BuOO$^{\bullet}$ is too slow to compete with its dimerization, then, in the presence of a high concentration of DEPMPO most of the *tert*-BuO$^{\bullet}$ radicals should be trapped before their β-scission thus leading to DEPMPO–O*tert*-Bu. Our assumption was confirmed by the generation of an authentic sample of DEPMPO-O*tert*-Bu in phosphate buffer–*tert*-butanol (10/1 v/v). The spin adduct was first generated in *tert*-butanol (a_P = 4.69 mT, a_N = 1.33 mT and $a_{H\beta}$ = 0.89 mT) by UV-photolysis of (*tert*-BuO)$_2$ in the presence of DEPMPO. After dilution in phosphate buffer (1/10 v/v), the $a_{H\beta}$ coupling changed dramatically, and a spectrum composed of a doublet (a_P = 4.65 mT) of quadruplets (a_N = 1.39 mT; a_H = 1.46 mT) was observed (Fig. S2d‡). The spectrum shown in Fig. 4c was then satisfactorily calculated assuming the superimposition of the DEPMPO–OOMe (60%) and DEPMPO–O*tert*-Bu (40%) signals. It is noteworthy that even at low concentration (10 mM) of DEPMPO a small amount of DEPMPO–O*tert*-Bu is generated, and the spectrum shown in Fig. 4a was satisfactorily calculated assuming the superimposition of the DEPMPO–OOMe (95%) and DEPMPO–O*tert*-Bu (5%) signals. When the decomposition of *tert*-BuOOH with chloroperoxidase was performed under oxygen-free conditions, the formation of DEPMPO–OOMe was avoided (Fig. 4b).

Trapping of linoleic acid peroxyl radical. A solution containing 13-hydroperoxylinoleic acid (LOOH) (0.15 M) prepared according to Martini *et al.*[33] and DEPMPO (50 mM) in deoxygenated phosphate buffer (0.1 M, pH 7.4) appeared not totally ESR silent, showing a weak signal (Fig. 5a).

Addition of cytochrome c (25 μM) to this reaction mixture led to the observation of an intense and complex ESR signal with a pattern similar to that of a peroxyl adduct (Fig. 5b). Calculation showed that this signal corresponded to the superimposition of the signals of DEPMPO–OOL (93.5%) and DEPMPO–OH (6.5%) spin adducts, the parameters of which are given in Table 1. After 30 min incubation, the original spectrum had evolved into a different pattern (Fig. 5c) corresponding to the superimposition of two signals: a doublet of quadruplet (**+**, Fig. 5c) assigned to DEPMPO–OH and a poorly resolved multiplet (×, Fig. 5c) (a_N = 1.49; a_P = 4.77 and $a_{H\beta}$ = 2.24 mT) assigned to an adduct (DEPMPO–L) resulting from the trapping of a carbon-centered radical deriving from the decomposition of LOO$^{\bullet}$.

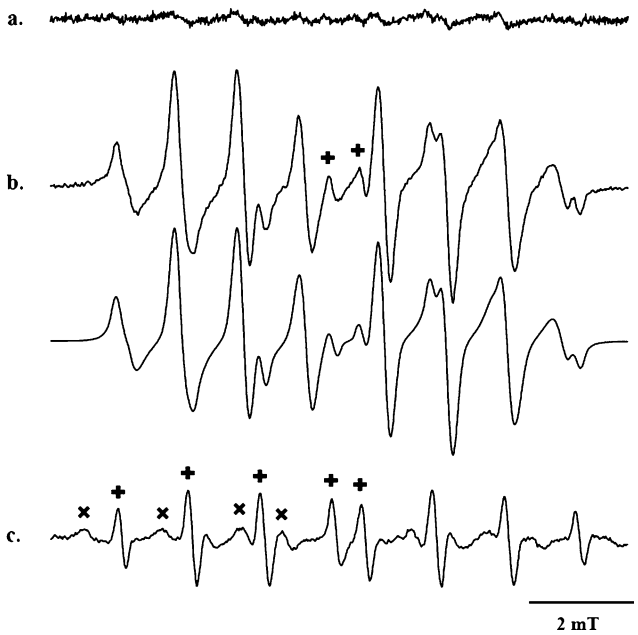

Fig. 5 DEPMPO–OOL spin adduct formation *via* the cytochrome c system. a. Incubation mixture containing DEPMPO (25 mM) and LOOH (0.15 M) in deoxygenated phosphate buffer (0.1 M, pH 7.4), **b.** as **a.** but after adding cytochrome c (20 μM). The signal below represents the simulation **c.** Remaining signal obtained after 30 min of incubation. Spectrometer settings: microwave power, 20 mW; modulation amplitude, 0.1 mT; time constant, 0.128 s; gain, 5×10^4; scan range, 12 mT and scan time, 46 s (4 scans for **c.**).

Discussion

In this work, various alkyl peroxyl radicals: $CH_3OO^{\bullet}$, *n*-BuOO$^{\bullet}$, *i*-PrOO$^{\bullet}$ and LOO$^{\bullet}$ were generated in phosphate buffer and efficiently trapped by DEPMPO to afford easily observable ESR spectra. These spectra exhibited significantly different ESR patterns in comparison with the corresponding authentic DEPMPO–alkoxyl adducts (Fig. 2). As far as we know, among the commonly used spin traps, DEPMPO is the only one which allows the unambiguous detection and characterization of alkylperoxyl radicals ROO$^{\bullet}$ (R = Me, primary alkyl and secondary alkyl) either in water or organic solvents. The formation of $CH_3OO^{\bullet}$, *n*-BuOO$^{\bullet}$ and *i*-PrOO$^{\bullet}$ from the Fenton reaction in the presence of the corresponding dialkylsulfoxides and O_2 is straightforward and the assignments of the observed EPR spectra were clearly supported by the results obtained on changing the experimental conditions, and the similitude of the calculated coupling constants with those determined in organic solvents.

Our attempts to obtain an unambiguous characterization of the trapping of tertiary alkylperoxyl radicals in water with DEPMPO failed, and only the tertiary alkoxyl radicals were trapped. Thus, either the rate of trapping of tertiary alkylperoxyl radicals is too slow to compete with their dimerization to tetraoxide or the corresponding spin adducts are very short lived and decompose quickly generating the tertiary alkoxyl radical adduct.

Several authors reported on their attempts to trap polyunsaturated fatty acid (PUFA) peroxyl radicals.[20,34–37] However, the complexity of the lipid radical chemistry, which includes β-scission, 1,2-radical shift and cyclisation of the alkoxyl radicals makes difficult the detection and unambiguous assignment of lipid-derived free radicals. The reported PUFA peroxyl radical adducts observed during the reduction of peroxidized PUFA with lipoxygenase in the presence of DMPO were unambiguously reassigned to PUFA alkoxyl radical adducts.[20] In the presence of DEPMPO or various EMPO derivatives, Stolze *et al.* were not able to unambiguously characterize the trapping of a PUFA peroxyl radical.[38]

In our work, decomposition with cytochrome c of linoleic acid hydroperoxide (LOOH), prepared according to Martini *et al.*'s

procedure,[33] was used to generate the secondary peroxyl radical, LOO$^{\bullet}$ in water. In the presence of DEPMPO, we obtained an ESR signal similar to that observed with *i*-PrOO$^{\bullet}$ exhibiting an alternated line width phenomenon. This ESR spectrum can be satisfactorily calculated assuming a chemical exchange between two conformational sites with different ESR hyperfine coupling constants. After 30 min of incubation, the main remaining signal is a doublet of 1/2/2/1 quadruplet assigned to the hydroxyl spin adduct (DEPMPO–OH) which could be formed either by the breakdown of the O–O bond during LOOH reduction by Fe^{2+} (Cytc-Fe^{2+}) or by Fe^{3+}-catalyzed nucleophilic addition of water. The detection of a carbon-centered radical spin adduct (DEPMPO–L) agrees with the observation of Dikalov and Mason.[20]

During spin trapping experiments involving *tert*-BuOOH and either chloroperoxidase or cytochrome c in the presence of DEPMPO, we unambiguously detected the formation of DEPMPO–$OOCH_3$ adducts, however we never observed the DEPMPO–OCH_3 spin adduct as was reported with DMPO by many authors.[19,20] The study of the reactions involving *tert*-BuOOH with chloroperoxidase or cytochrome c confirmed that the DEPMPO–OO*tert*-Bu adduct cannot be detected in aqueous medium. Either the rate of trapping of *tert*-BuOO$^{\bullet}$ is too low to compete with its dimerization to a transient tetraoxide or the DEPMPO–OO*tert*-Bu is too short-lived to be detected. Then, fragmentation of the tetraoxide and DEPMPO–OO*tert*-Bu will generate *tert*-BuO$^{\bullet}$ radicals which decompose into acetone and $CH_3^{\bullet}$ radicals. In the presence of oxygen, $CH_3^{\bullet}$ radicals generate $CH_3OO^{\bullet}$ radicals which are trapped with DEPMPO.

Conclusion

Various alkylperoxyl radicals ROO$^{\bullet}$ (R = Me, *n*-Bu, *i*-Pr) have been produced in water and trapped with DEPMPO to generate DEPMPO–OOR adducts which were easily detected by ESR. As for DEPMPO–OOH, the ESR signals of DEPMPO–OOR spin adducts exhibit a pattern characteristic of the existence of a chemical exchange between two conformational sites. With DEPMPO we were able to characterize the spin adduct DEPMPO–OOL, resulting from the trapping of the secondary alkylperoxyl radical obtained by reduction of 13-hydroperoxylinoleic acid, LOOH. Attempts to trap tertiary alkyl peroxyl radicals resulted in the observation of tertiary alkoxyl spin adducts.

Unlike DMPO and EMPO and various analogs, our results establish that DEPMPO can be a useful tool to characterize the alkylperoxyl radicals generated from organic hydroperoxides or lipid peroxidation.

Experimental

Chemicals

Xanthin oxidase (XOD) and bovine erythrocyte superoxide dismutase (SOD) were purchased from Boehringer Mannheim Biochemical Co. Cytochrome c from horse heart, chloroperoxidase (1300 U.mg^{-1} protein) from *Caldariomyces fumago*, glutathione (GSH), glutathione peroxidase (Gpx), diethylenetriaminepentaacetic acid (DTPA), *tert*-butylhydroperoxide, and other chemicals were from Sigma Chemical Co. DEPMPO was supplied by Radical Vision, Marseilles, France. Dialkylsulfoxides (nBu$_2$SO and iPr$_2$SO) were prepared according to Kakarla and Sofia.[39]

ESR measurements

ESR spectra were recorded at room temperature using a Bruker ESP 300 ESR spectrometer at 9.5 GHz (X-band) employing 100 kHz field modulation. Reaction mixtures were prepared in a chelex-treated phosphate buffer (0.1 M, pH 7.4). Standard ESR spectra were simulated using the ESR software developed by D. Duling from the Laboratory of Molecular Biophysics, NIEHS, USA.§ ESR spectra were also simulated with ROKI, a computer simulation program developed by Rockenbauer[40] that uses an automatic fitting procedure based also on optimization of the exchange rate between potential conformers. The UV-photolysis was performed by a 1000 W UV Xe–Hg Oriel lamp (Newport Corp., CA, USA).

Spin trapping experiments

All the given concentrations are final concentrations in the different reaction mixtures described.

ROO$^{\bullet}$ generation from dialkylsulfoxide. ROO$^{\bullet}$ radicals were generated by UV-photolysis of a solution containing R_2SO (10%), H_2O_2 (1% v/v) and DEPMPO (5 mM) in oxygen-saturated phosphate buffer (0.1 M, pH 7.4). Dibutyl and diisopropylsulfoxide were prepared according to a published procedure.[39]

Reaction of cytochrome c with *tert*-BuOOH. Cytochrome c (20 μM) was added to a deoxygenated phosphate buffer (0.1 M, pH 7.4) solution containing *tert*-BuOOH (15 mM) and DEPMPO (5 to 50 mM).

Reaction of chloroperoxidase with *t*-BuOOH. Chloroperoxidase (10 U mL^{-1}) was incubated for 4 min in an oxygenated phosphate buffer (0.1 M, pH 7.4) solution containing DEPMPO (10 or 100 mM) and *tert*-BuOOH (60 mM).

ROO$^{\bullet}$ generation from 2,2′-azobis-2-methylpropionamidine (AAPH). The protonated 2-methylpropionamidinylperoxyl radical (AAPH-OO$^{\bullet}$) was generated by UV-photolysis of an oxygen-saturated phosphate buffer (0.1 M, pH 7.4) solution of AAPH (10 mM) and DEPMPO (25 mM).

Reaction of cytochrome c with 13-hydroperoxylinoleic acid (LOOH). Cytochrome c was added (20 μM) to an oxygenated phosphate buffer (0.1 M, pH 7.4) solution containing LOOH (15 mM) and DEPMPO (25 mM).

DEPMPO–OR formation. These spin adducts were obtained in water by addition of 30 μL of a ROH solution containing $FeCl_3$ (2 mM) and DEPMPO (0.5 M) to 270 μL of phosphate buffer (0.1 M, pH 7.4) containing DTPA (20 mM).[20,41]

The DEPMPO–O*tert*-Bu spin adduct was generated in water by irradiating a solution of (*tert*-BuO)$_2$ (0.5 M) and DEPMPO (50 mM) in *tert*-butanol followed by 1/10 dilution in phosphate buffer (0.1 M, pH 7.4).

Addition of Fe^{2+} (0.5 mM) to a deoxygenated phosphate buffer solution (0.1 M, pH 7.4) containing *tert*-BuOOH (4 mM)

§ This software is available *via* the World Wide Web at http://www.niehs.nih.gov/research/resources/software/tools/index.cfm

and DEPMPO (0.05 M) led to a mixture of DEMPO-O*tert*-Bu (73%) and DEPMPO-CH_3 (27%) (see Electronic Supplementary Information, Fig. S4‡).

List of abbreviations.

DMPO	2,2-dimethyl-3,4-dihydro-2*H*-pyrrole 1-oxide
DEPMPO	2-(diethoxyphosphoryl)-2-methyl-3,4-dihydro-2*H*-pyrrole 1-oxide
PUFA	Polyunsaturated fatty acid
ESR	Electron spin resonance
ROO$^{\bullet}$	Peroxyl free radical
LOO$^{\bullet}$	Linoleic acid peroxyl free radical
RO$^{\bullet}$	Alkoxyl free radical
DTPA	Diethylenetriaminepentaacetic acid
tert-BuOOH	*tert*-butyl hydroperoxide
LOOH	13-hydroperoxylinoleic acid
AAPH	2,2′azobis-2-methyl-propionamidine hydrochloride

Acknowledgements

We thank Professor Antal Rockenbauer for providing us with the computer simulation program and for helpful discussions. We also thank Dr Micael Hardy for the kind gift of linoleic acid hydroperoxide and Radical Vision for the generous supply of DEPMPO spin trap.

Notes and references

1 H. Wiseman and B. Halliwell, *Biochem. J.*, 1996, **313**, 17.
2 K. Keyer and J. A. Imlay, *Proc. Natl. Acad. Sci. U. S. A.*, 1996, **93**, 13635.
3 J. A. Berliner and J. W. Heinecke, *Free Radical Biol. Med.*, 1996, **20**, 707.
4 R. T. Dean, S. Fu, R. Stocker and M. J. Davies, *Biochem. J.*, 1997, **324**, 1.
5 S. Fu, M. J. Davies, R. Stocker and R. T. Dean, *Biochem. J.*, 1998, **333**, 519.
6 (*a*) B. Kalyanaraman, C. Mottley and R. P. Mason, *J. Biol. Chem.*, 1983, **258**, 3855; (*b*) W. Chamulitrat and R. P. Mason, *J. Biol. Chem.*, 1989, **264**, 20968.
7 J. A. Degray and R. P. Mason, Biological spin trapping, *Electron Spin Resonance*, 1994, **14**, 246.
8 M. J. Davies, Recent developments in EPR-spin trapping, *Electron Spin Resonance*, 2002, **18**, 47.
9 J.-L. Clement and P. Tordo, Advances in Spin-trapping, *Electron Spin Resonance*, 2007, **20**, 29.
10 E. Finkelstein, G. M. Rosen and E. J. Rauckman, *J. Am. Chem. Soc.*, 1980, **102**, 4994.
11 M. J. Davies., *Biochim. Biophys. Acta, Gen. Subj.*, 1988, **964**, 28.
12 W. Chamulitrat, N. Takahashi and R. P. Mason, *J. Biol. Chem.*, 1989, **264**, 7889.
13 M. J. Davies, *Biochim. J.*, 1989, **257**, 603.
14 M. J. Davies, *Free Radical Res.*, 1989, **7**, 27.
15 D. P. Barr and R. P. Mason, *J. Biol. Chem.*, 1995, **270**, 12709.
16 J. Van Der Zee, D. P. Barr and R. P. Mason, *Free Radical Biol. Med.*, 1996, **20**, 199.
17 V. Misik and P. Riesz, *Free Radical Biol. Med.*, 1996, **20**, 129.
18 J. Van Der Zee, *Biochim. J.*, 1997, **322**, 633.
19 S. I. Dikalov and R. P. Mason, *Free Radical Biol. Med.*, 1999, **27**, 864.
20 S. I. Dikalov and R. P. Mason, *Free Radical Biol. Med.*, 2001, **30**, 187.
21 C. M. Jones and M. J. Burkitt, *J. Chem. Soc., Perkin Trans. 2*, 2002, (12), 2044.
22 C. Fréjaville, H. Karoui, F. Le Moigne, M. Culcasi, S. Piétri, R. Lauricella, B. Tuccio and P. Tordo, *J. Med. Chem.*, 1995, **38**, 258.
23 A. Muller, S. Pietri, M. Villain, C. Fréjaville, C. Bonne and M. Culcasi, *Exp. Eye Res.*, 1997, **64**, 637.
24 J. Vasquez-Vivar, B. Kalyanaraman, P. Martasek, N. Hogg, B. S. Masters, H. Karoui, P. Tordo and K. A. Pritchard Jr, *Proc. Natl. Acad. Sci. U. S. A.*, 1998, **95**, 9220.
25 V. Roubaud, S. Sankarapandi, P. Kuppusamy, P. Tordo and J. L. Zweier, *Anal. Biochem.*, 1998, **257**, 210.
26 H. P. Souza, L. C. Souza, V. M. Anastacio, A. C. Pereira, M. de L. Junqueira, J. E. Krieger, P. L. Da Luz, O. Augusto and F. R. M. Laurindo, *Free Radical Biol. Med.*, 2000, **28**, 1232.
27 O. Inanami, T. Yamamori, T. A. Takahashi, H. Nagahata and M. Kuwabara, *Free Radical Res.*, 2001, **34**, 81.
28 C Fréjaville, H. Karoui, F. Le Moigne, M. Culcasi, S. Piétri, R. Lauricella, B. Tuccio and P. Tordo, *J. Chem. Soc., Chem. Commun.*, 1994, 1793.
29 J.-L. Clément, J.-P. Finet, C. Fréjaville and P. Tordo, *Org. Biomol. Chem.*, 2003, **1**, 1591.
30 J.-L. Clément, B. C. Gilbert, A. Rockenbauer, P. Tordo and A. C. Whitwood, *Free Radical Res.*, 2002, **36**, 883.
31 P. Stocker, J. F. Lesgards, N. Vidal, F. Chalier and M. Prost, *Biochim. Biophys. Acta, Gen. Subj.*, 2003, **1621**, 1.
32 R. D. Hall, W. Chamulitrat, N. Takahashi, C. F. Chignell and R. P. Mason, *J. Biol. Chem.*, 1989, **264**, 7900.
33 D Martini, G. Iacazio, D. Ferrand, G. Buono and C. Triantaphilides, *Biocatal. Biotransform.*, 1994, **11**, 47.
34 K Stolze, N. Udilova and H. Nohl, *Biochem. Pharmacol.*, 2002, **63**, 1465.
35 K. Stolze, N. Udilova, T. Rosenau, A. Hofinger and H. Nohl, *Biochem. Pharmacol.*, 2003, **66**, 1717.
36 K Stolze, N. Udilova, T. Rosenau, A. Hofinger and H. Nohl, *Biochem. Pharmacol.*, 2004, **68**, 185.
37 K. Stolze, N. Udilova, T. Rosenau, A. Hofinger and H. Nohl, *Biochem. Pharmacol.*, 2005, **69**, 297.
38 K. Stolze, N. Udilova and H. Nohl, *Free Radical Biol. Med.*, 2000, **29**, 1005.
39 R. Kakarla, R. G. Dulina, N. T. Hatzenbuhler, Y. W. Hui and M. J. Sofia, *J. Org. Chem.*, 1996, **61**, 8347.
40 A. Rockenbauer and L. Korecz, *Appl. Magn. Reson.*, 1996, **10**, 29.
41 P. M. Hanna, W. Chamulitrat and R. P. Mason, *Arch. Biochem. Biophys.*, 1992, **296**, 640.

